scientific reports

Check for updates

OPEN

Electroencephalography and optical neuromonitoring predict short-term outcomes in neonates undergoing therapeutic hypothermia for hypoxic-ischemic encephalopathy

Rasheda Arman Chowdhury[1,2]✉, Zamzam Mahdi[1], Beatrice Desnous[1,3], Bohdana Marandyuk[1], Ala Birca[1,3], Ramy El-Jalbout[1,4], Anne-Monique Nuyt[1,5], Elana F. Pinchefsky[1,3,6] & Mathieu Dehaes[1,2,4,6]✉

Electroencephalography (EEG) and optical neuromonitoring were used to predict short-term outcomes in neonates undergoing therapeutic hypothermia (TH) for hypoxic-ischemic encephalopathy (HIE). Fifty-two neonates undergoing TH for HIE were prospectively recruited. Continuous EEG monitoring was initiated within 24 h of life and a quantitative discontinuity index was calculated. Combined frequency-domain near infrared spectroscopy (FDNIRS) and diffuse correlation spectroscopy (DCS) were initiated within 48 h of life and used to measure cerebral hemoglobin oxygen saturation (SO_2) and a cerebral blood flow index. Using these parameters and hemoglobin concentration measurements, cerebral oxygen extraction fraction (OEF), indices of cerebral oxygen delivery and metabolism ($CMRO_{2i}$) as well as cerebral oxygen reserve (CRO_2) were derived. Short-term outcome was classified based on brain injury pattern on magnetic resonance imaging and/or death; as normal-mild, moderate or severe outcome. Results showed that EEG discontinuity index, SO_2 and CRO_2 were higher and OEF lower in neonates with severe compared to normal-mild and moderate outcomes during TH. EEG discontinuity index was the most accurate and earliest parameter to identify moderate *vs.* severe outcomes while $CMRO_{2i}$ identified normal-mild *vs.* moderate outcomes as early as day 2 of TH. Combining EEG and FDNIRS-DCS parameters improved area-under-the-curve, sensitivity and specificity for most of the predictive models.

Keywords Hypoxic-ischemic encephalopathy (HIE), Electroencephalography (EEG), Frequency-domain near infrared spectroscopy (FDNIRS), Diffuse correlation spectroscopy (DCS), Magnetic resonance imaging (MRI), Predictive models

Hypoxic-ischemic encephalopathy (HIE) is the leading cause of death and neurological sequelae in term and near-term neonates[1–4]. Therapeutic hypothermia (TH) is currently the only effective treatment that has significantly decreased mortality rates and major neurodevelopmental disability in moderate to severe neonatal HIE[5–7]. Despite TH, adverse neurodevelopmental outcome remains frequent in survivors[8]. Hypoxic-ischemic brain injury evolves over hours to days and is associated with specific neurophysiological and cerebral perfusion changes[9–11]. The initial hypoxic-ischemic insult triggers oxidative stress, and subsequent hyperperfusion

[1]Research Center, CHU Sainte-Justine University Hospital Centre, 3175 Cote Sainte-Catherine, Montreal, QC H3T1C5, Canada. [2]Institute of Biomedical Engineering, Université de Montréal, Montreal, QC, Canada. [3]Division of Neurology, Department of Neurosciences and Paediatrics, Université de Montréal, Montreal, QC, Canada. [4]Department of Radiology, Radio-Oncology and Nuclear Medicine, Université de Montréal, Montreal, QC, Canada. [5]Division of Neonatology, Department of Paediatrics, Université de Montréal, Montreal, QC, Canada. [6]Elana F. Pinchefsky and Mathieu Dehaes jointly supervised this work. ✉email: rasheeda.arman@gmail.com; mathieu.dehaes@umontreal.ca

exacerbates this stress by promoting inflammation and reactive oxygen species production. This cascade of events contributes to the severity of neuronal injury and influences the clinical outcomes[11]. Previous studies showed that TH delays the occurrence of cerebral hyperperfusion in brain areas exhibiting injury to day 2–3[10,12]. Measurements of these cerebral changes over the first days of life may be valuable prognostic markers of the severity and progression of HIE[13–16].

Prognostic characteristics of neuromonitoring have been previously studied as it may improve intensive care management of neonates with HIE undergoing TH and aid parental counseling. Neuromonitoring techniques include electroencephalography (EEG), amplitude-integrated EEG (aEEG), conventional near infrared spectroscopy (NIRS), and magnetic resonance imaging (MRI). Qualitative and quantitative EEG pattern analysis and conventional NIRS measures of regional cerebral oxygen saturation ($rScO_2$) and cerebral fractional tissue oxygen extraction (cFTOE) have been considerably studied as bedside biomarkers. These measures demonstrated early predictive value for both short-term (brain injury on MRI) and long-term neurodevelopment outcomes. EEG and NIRS parameters alone were predictive at different and specific times after initiation of TH. Studies have shown the predictive value of EEG was better after 24 h of life[17–19] whereas cerebral oxygenation measures were predictive only 24-72 h after birth depending on the study[19–22]. Combining the two modalities also showed improved predictive ability and at an earlier stage of TH[19–21,23–25]. A previous study using combined $rScO_2$ and aEEG background pattern could identify adverse outcome as early as 12 h after birth[21]. Quantitative EEG features may further improve early prediction of brain injury[26,27].

Previous studies have shown $rScO_2$ alone is useful for monitoring severity of the primary insult, yet the combination of frequency-domain NIRS (FDNIRS) and diffuse correlation spectroscopy (DCS) may improve sensitivity to identify evolving brain injury[28]. Cerebral perfusion and metabolism increase in an effort to stabilize $rScO_2$ during the evolution of brain injury and during brain development[28,29]. There is likely an additional effect of hypothermia on cerebral perfusion and oxygen metabolism, in addition to the effect of the hypoxic-ischemic injury[15]. These cerebral changes may potentially be assessed with FDNIRS-DCS, which measure absolute cerebral hemoglobin oxygen saturation (SO_2) and an index of cerebral blood flow (CBF_i), respectively[30,31]. When combined with arterial oxygen saturation (SaO_2) and hemoglobin concentration in the blood (HGB), these parameters allow to derive indices of cerebral metabolic rate of oxygen consumption ($CMRO_{2i}$) and oxygen delivery (CDO_{2i}) as well as cerebral oxygen reserve (CRO_2)[28,30–33]. In a previous study, lower $CMRO_{2i}$ and CBF_i during TH were observed compared to post-TH values and healthy control neonates suggesting a potential action of TH on cerebral hemodynamics and metabolism[34]. In an MRI study, cerebral perfusion was also related to HIE severity, being lower in severe compared to moderate HIE during the first 72 h after birth[15]. These studies show the potential value of cerebral hemodynamics and metabolism as predictive markers of outcome in neonatal HIE.

Prognostication of moderate encephalopathy in HIE is particularly challenging and prognostic models are sparse in the literature[35]. In the current study, continuous EEG and intermittent FDNIRS-DCS neuromonitoring were used to assess changes in cerebral electrical activity, oxygenation and metabolism in neonates with HIE during TH, rewarming and post-TH. We hypothesized that the combination of these techniques would improve early prognostic accuracy for the severity of brain injury/death compared to either method used alone. We further hypothesized that this approach would help to differentiate normal-mild, moderate, and severe short-term outcomes.

Results

Demographics, clinical and neuromonitoring characteristics

Demographic and clinical characteristics of the population (N = 52, male 60%) are summarized in (Table 1). Median gestational age was 39 weeks and 2 days (IQR 38–40) and median birth weight was 3.5 kg (IQR 2.8–3.7). All patients had MRI scans available for review except for one who died at 4 days of age after redirection of care. Three neonates (6%) died prior to hospital discharge. One of them had no injury identified on MRI on day 5 of life. These three patients were classified in the severe outcome group. In total, thirty-three (63%) neonates were classified as normal-mild, 9 (17%) as moderate, and 10 (20%) as severe short-term outcomes based on MRI pattern of injury or death before discharge (Supplementary Table S1). Based on the initial Sarnat examination, 4 patients (7.7%) were graded as mild, 43 (82.7%) as moderate, and 5 (9.6%) as severe encephalopathy. Of those neonates who had severe short-term outcomes, 3 (30%) had severe encephalopathy and 7 (70%) moderate encephalopathy. The incidence of EEG confirmed seizures was significantly higher in the severe compared to the normal-mild and moderate outcome groups. The proportion of neonates who were delivered through emergency caesarian section and who were on mechanical ventilation during their hospitalization were significantly higher in the severe compared to the normal-mild outcome group. The median age at full oral feed was also significantly different between the severe and normal-mild outcome group. Boxplot distribution of FDNIRS-DCS variables across measurement locations is provided in (Supplementary Fig. S1).

EEG discontinuity and FDNIRS-DCS parameters classified by short-term outcomes

Figure 1 shows EEG discontinuity index in patients with normal-mild, moderate and severe short-term outcomes during TH day 1 (TH1), day 2 (TH2), day 3 (TH3), rewarming (Rewarm) and post-therapeutic hypothermia (Post-TH). EEG discontinuity index was higher in the severe group compared to moderate and normal-mild groups during TH1 and TH2 periods. EEG discontinuity index remained higher in the severe group compared to the moderate group during TH3. No significant differences in EEG discontinuity index were observed between moderate and normal-mild groups nor during rewarming and post-TH.

Figure 2 shows SO_2, oxygen extraction fraction (OEF) and CRO_2 in patients with normal-mild, moderate and severe short-term outcomes during TH2, TH3, Rewarm, Post-TH, and before discharge (Pre-DC) periods. The severe group compared to the normal-mild group had higher SO_2 and CRO_2 while OEF was lower during

Clinical characteristics	Full cohort (N = 52)	Normal-mild outcome (N = 33)	Moderate outcome (N = 9)	Severe outcome (N = 10)
Gestational age, weeks	39.2 (38.1, 40.4)	38.6 (38, 40.3)	40 (38.2, 40.5)	40 (38, 40.6)
Weight, kg	3.5 (2.8, 3.7)	3.5 (2.9, 3.7)	3.5 (2.8, 3.6)	3.4 (2.7, 3.9)
Male sex	31 (60)	19 (57.6)	7 (77.8)	5 (50)
Emergent caesarian section	23 (44)	**12 (36.4)***	3 (33.3)	**8 (80)***
Apgar score, 5 min	4 (3, 5)	4 (3, 5)	4 (2, 6)	3 (2, 4)
Apgar score, 10 min	5 (4, 6)	5 (4, 6)	4 (3, 6)	4 (4, 4)
Resuscitation score[a]	3 (3, 4)	3 (3, 4)	4 (3, 5)	4 (3, 5)
Sarnat stage at admission				
Mild	4 (7.7)	3 (9.1)	1 (11.1)	0 (0)
Moderate	43 (82.7)	29 (87.9)	7 (77.8)	7 (70)
Severe	5 (9.6)	1 (3)	1 (11.1)	3 (30)
Umbilical arterial cord pH or worst arterial pH within the first hour of life[b]	6.9 (6.8, 7)	6.9 (6.8, 7)	6.9 (6.7, 6.9)	6.8 (6.9, 7.1)
Umbilical arterial cord base excess or worst base excess within the first hour of life	17 (13.6, 22.3)	17 (13, 20)	22.5 (16.9, 25)	15 (13.5, 20)
Maximum lactate value	9.6 (5.4, 15.4)	7.9 (5, 13.6)	14.4 (8.2, 18)	14.2 (8.6, 17.9)
Suspicion of clinical seizures	24 (46)	13 (39.4)	3 (33.3)	8 (80)
aEEG/EEG confirmed seizures	12 (23)	**4 (12.1)***	**1 (11.1)†**	**7 (70)*†**
Received vasopressors	15 (29)	9 (27.3)	2 (22.2)	4 (40)
Number of patients on mechanical ventilation	35 (67.3)	**17 (51.5)***	8 (88.9)	**10 (100)***
Days on ventilator	4 (2, 5)	4 (1.5, 5.5)	3 (1, 4)	4 (2.8, 5)
Age at full oral feed, days[c]	8.5 (6, 14)	**8 (6, 11.2)***	13 (6, 19)	**18 (15.5, 20)***
Length of hospital stay, days	11 (7, 17)	10 (7, 14.5)	13 (6, 20)	19 (10, 20.3)
Age at pre-discharge FDNIRS-DCS monitoring, days	7 (6, 13)	7 (6, 14)	8 (6, 12)	7 (5, 16)
Age at MRI, days	5 (4, 6)	5 (4, 6)	4 (3, 6)	5 (4,7)

Table 1. Clinical characteristics and demographics. Data are presented for the full cohort as well as for normal-mild, moderate and severe short-term outcome groups. Data are described as median (interquartile range IQR), or frequency (%). *MRI:* magnetic resonance imaging, *FDNIRS:* frequency domain near infrared spectroscopy, *DCS:* diffuse correlation spectroscopy, *EEG:* electroencephalography, *aEEG:* amplitude-integrated EEG. [a]Score ranging from 1 (no intervention) to 6 (endotracheal intubation and epinephrine)[97]. [b]First hour arterial blood gas was used when umbilical arterial cord gas was not available. [c]No patients required nasogastric feeds at discharge. *$p < 0.05$ for comparisons between normal-mild and severe outcome groups. †$p < 0.05$ for comparisons between moderate and severe outcome groups.

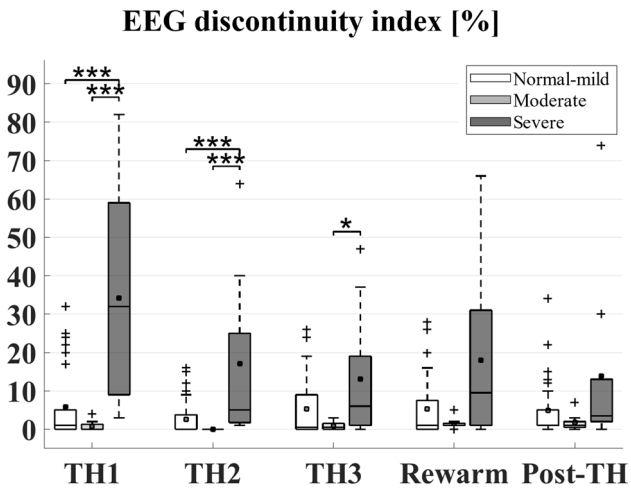

Fig. 1. Boxplot representation of the EEG discontinuity index in patients with normal-mild (white), moderate (light gray) and severe (dark gray) short-term outcomes during therapeutic hypothermia day 1 (TH1), day 2 (TH2), day 3 (TH3), rewarming (Rewarm) and post-therapy (Post-TH). Mean, median and outliers are represented by squares (▪), lines (▬) and plus (+) symbols, respectively. *$p < 0.05$; **$p < 0.01$; ***$p < 0.001$.

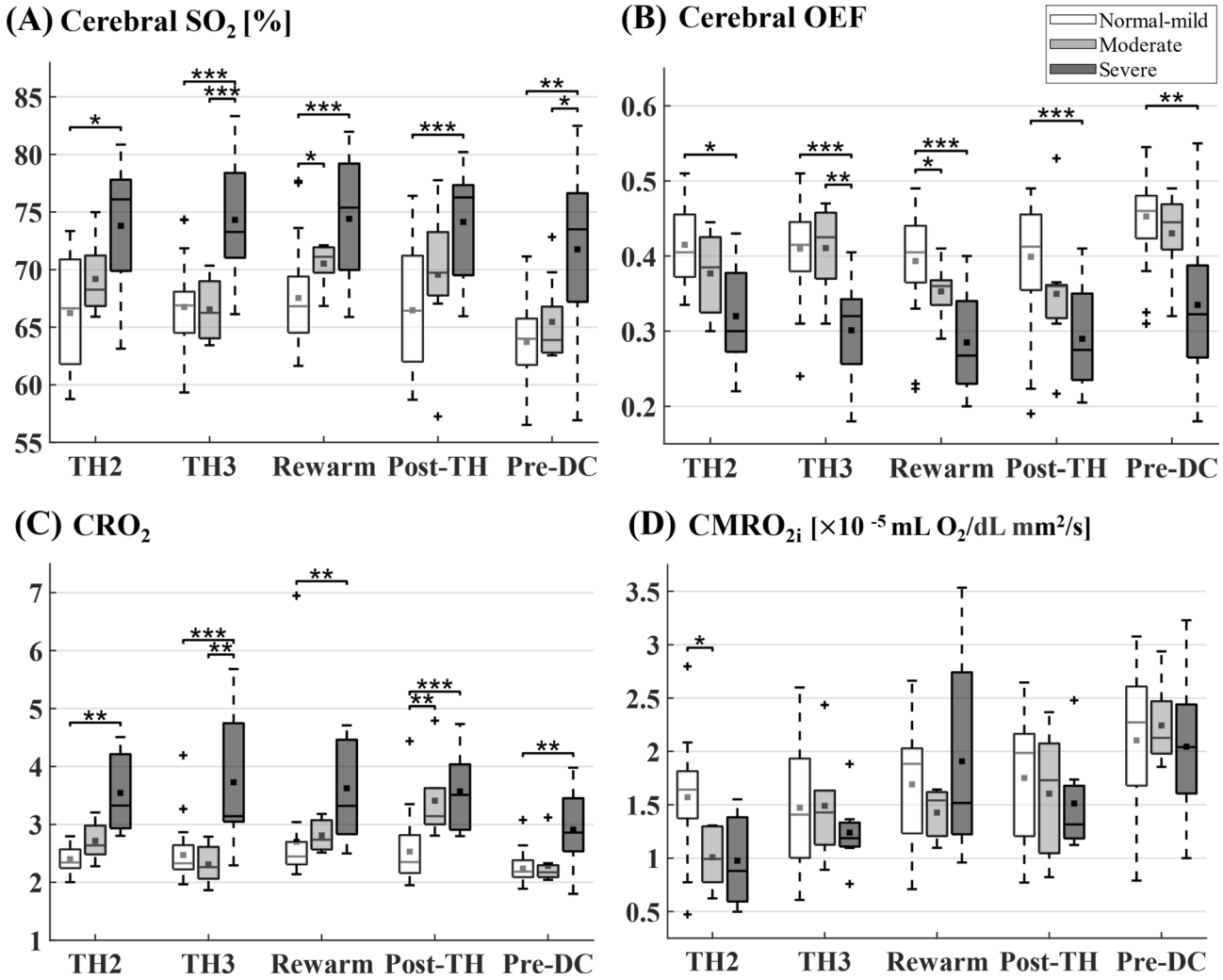

Fig. 2. Boxplot representation of (**A**) cerebral oxygen hemoglobin saturation (SO_2), (**B**) cerebral oxygen extraction fraction (OEF), (**C**) cerebral oxygen reserve (CRO_2), and (**D**) cerebral metabolic rate of oxygen consumption ($CMRO_{2i}$) in HIE neonates with normal-mild (white), moderate (light gray) and severe (dark gray) short-term outcomes during therapeutic hypothermia day 2 (TH2), day 3 (TH3), rewarming (Rewarm), post-therapy (Post-TH) and before discharge (Pre-DC). Mean, median and outliers are represented by squares (▪), lines (▬) and plus (+) symbols, respectively. *$p < 0.05$; **$p < 0.01$; ***$p < 0.001$.

all periods of neuromonitoring. Similar patterns were observed in moderate compared to normal-mild group during rewarming (significant for SO_2 and OEF only) and post-TH (significant for CRO_2 only). The severe group compared to the moderate group had higher SO_2 and CRO_2 with lower OEF during TH3 and pre-discharge periods (non-significant for CRO_2 and OEF with $p = 0.054$). The moderate group compared to the normal-mild group also presented lower $CMRO_{2i}$ ($p = 0.045$) during TH2. No significant differences in CDO_{2i} were found, except during rewarming a tendency towards a higher CDO_{2i} in severe group compared to normal-mild group ($p = 0.084$) was observed (Supplementary Fig. S2).

Prediction of short-term outcomes

The performance of statistical models using EEG discontinuity index, FDNIRS-DCS parameters, and the combination of both to predict moderate vs. severe short-term outcomes are shown in (Table 2). For each model, optimal cut-off, area under the receiver operating characteristics (ROC) curve, 95% confidence intervals (CI), sensitivity (Se), and specificity (Sp) are presented. During TH2, EEG discontinuity index and CRO_2 predicted the outcome with good accuracy (area under the ROC curve [AUC] > 0.8) while during TH3 all parameters showed good predictive accuracy (except $CMRO_{2i}$ and CDO_{2i}). During rewarming, EEG discontinuity index, OEF and CDO_{2i} were significant predictors while none of the parameters showed a predictive value post-TH. Combining EEG discontinuity index with any FDNIRS-DCS parameters improved predictive accuracy compared to each parameter alone at all time periods.

Similarly, the performance of statistical models using EEG discontinuity index, FDNIRS-DCS parameters and combination of both to predict normal-mild vs. moderate outcomes was assessed (Table 3). EEG discontinuity

Periods	Predictive variables	EEG disc	CRO_2	SO_2	OEF	$CMRO_{2i}$	CDO_{2i}
TH2	Optimal cut-off	0.008	3.3	71.7	0.31	0.56	2.12
	AUC	**1*****	**0.87***	0.78	0.75	0.53	0.6
	[95% CI]	[1; 1]	[0.58; 1]	[0.43; 1]	[0.44; 0.1]	[0.3; 1]	[0.2; 1]
	Se/Sp (%)	100/100	100/66.7	87.5/80	60/87.5	33.3/100	100/40
TH3	Optimal cut-off	0.04	2.9	70.4	0.35	1.27	3.52
	AUC	**0.86*****	**0.93*****	**0.94*****	**0.88*****	0.64	0.76
	[95% CI]	[0.69; 1]	[0.77; 1]	[0.83; 1]	[0.71; 1]	[0.32; 0.96]	[0.49; 1]
	Se/Sp (%)	100/70	100/85.7	100/88.9	77.8/88.9	71.4/66.7	71.4/83.3
Rewarm	Optimal cut-off	0.06	3.23	73.2	0.31	1.75	3.89
	AUC	**0.83***	0.76	0.71	**0.77***	0.57	**0.86***
	[95% CI]	[0.62; 1]	[0.46; 1]	[0.45; 0.98]	[0.54; 1]	[0.19; 0.95]	[0.58; 1]
	Se/Sp (%)	100/70	100/71.4	100/60	70/85.7	42.9/100	100/66.7
Post-TH	Optimal cut-off	0.02	3.37	75.0	0.30	1.12	4.24
	AUC	0.73	0.54	0.70	0.71	0.51	0.51
	[95% CI]	[0.47; 0.98]	[0.19; 0.90]	[0.45; 0.95]	[0.47; 0.96]	[0.12; 0.9]	[0.15; 0.88]
	Se/Sp (%)	75/80	80/57.1	88.9/60	60/88.9	100/40	85.7/40
Periods	**Predictive variables**	**EEG disc x CRO_2**	**EEG disc x SO_2**	**EEG disc x OEF**	**EEG disc x $CMRO_{2i}$**	**EEG disc x CDO_{2i}**	
TH2	AUC	**1*****	**1*****	**1*****	**1*****	**1*****	
	[95% CI]	[1; 1]	[1; 1]	[1; 1]	[1; 1]	[1; 1]	
	Se/Sp (%)	100/100	100/100	100/100	100/100	100/100	
TH3	AUC	**1*****	**1*****	**0.98*****	**0.97*****	**0.89*****	
	[95% CI]	[1; 1]	[1; 1]	[0.93; 1]	[0.87; 1]	[0.69; 1]	
	Se/Sp (%)	100/100	100/100	85.7/100	83.3/100	71.4/100	
Rewarm	AUC	**1*****	**1*****	**1*****	**0.93*****	**0.85***	
	[95% CI]	[1; 1]	[1; 1]	[1; 1]	[0.74; 1]	[0.57; 1]	
	Se/Sp (%)	100/100	100/100	100/100	85.7/100	71.4/100	
Post-TH	AUC	**0.93*****	**0.89*****	**0.86*****	**0.96*****	**0.96*****	
	[95% CI]	[0.77; 1]	[0.72; 1]	[0.69; 1]	[0.86; 1]	[0.86; 1]	
	Se/Sp (%)	85.7/100	77.8/100	80/87.5	85.7/100	85.7/100	

Table 2. EEG discontinuity index and FDNIRS-DCS parameters used separately and combined as predictors of moderate *vs.* severe outcomes during therapeutic hypothermia day 2 (TH2), day 3 (TH3), rewarming (Rewarm) and post-therapy (Post-TH). Receiver operating characteristics (ROC) curve (AUC) analysis is presented with optimal cut-off, sensitivity, specificity, and the corresponding 95% confidence interval. *$p < 0.05$; **$p < 0.01$; ***$p < 0.001$. *FDNIRS-DCS:* frequency domain near infrared spectroscopy and diffuse correlation spectroscopy, *EEG*: electroencephalography, *TH:* therapeutic hypothermia, *TH2:* 42-48 h of age, *TH3:* last 6 h of TH, *Rewarm*: 0-6 h post-TH, *Post-TH:* 6-12 h post-TH, *Se:* Sensitivity, *Sp:* specificity, *CI:* confidence interval, *EEG disc:* EEG discontinuity index, CRO_2: cerebral oxygen reserve, SO_2: cerebral oxygen saturation, *OEF:* cerebral oxygen extraction fraction, $CMRO_{2i}$: cerebral metabolic rate of oxygen consumption, CDO_{2i}: cerebral oxygen delivery.

index alone showed poor accuracy for outcome prediction at all periods. $CMRO_{2i}$ was the only FDNIRS-DCS parameter that showed good predictive accuracy at TH2. CRO_2 reached good predictive accuracy during post-TH. The combination of EEG discontinuity index with CRO_2, $CMRO_{2i}$ and CDO_{2i} yielded good predictive accuracy during TH2. Combining EEG discontinuity index with CRO_2 and CDO_{2i} provided good predictive accuracy during rewarming and post-TH. The other combinations did not reach the standard for good accuracy. Performance to predict normal-mild vs. severe outcomes are provided in (Supplementary Table S2).

Discussion

We demonstrated that quantitative EEG and FDNIRS-DCS neuromonitoring, alone or combined, could serve as early predictors of normal-mild, moderate or severe short-term outcomes in neonates undergoing TH for HIE. During TH, the EEG discontinuity index, SO_2 and CRO_2 were higher while OEF was lower in neonates with severe outcomes compared to neonates with normal-mild and moderate outcomes. EEG discontinuity index was the most accurate and earliest parameter to identify moderate vs. severe short-term outcomes while $CMRO_{2i}$ helped differentiate normal-mild vs. moderate outcomes. For most predictive models, combining EEG discontinuity index and FDNIRS-DCS parameters improved AUC, sensitivity, and specificity. Some of these models allowed to differentiate normal-mild, moderate, and severe short-term outcomes with good accuracy and as early as day 2 of TH. To the best of our knowledge, this is the first study in neonates with HIE that

Periods	Predictive variables	EEG disc	CRO_2	SO_2	OEF	$CMRO_{2i}$	CDO_{2i}
TH2	Optimal cut-off	0.005	2.54	65.7	0.35	1.33	2.69
	AUC	0.59	**0.77***	0.68	0.68	**0.86*****	0.73
	[95% CI]	[0.41; 0.77]	[0.51; 1]	[0.49; 0.87]	[0.46; 0.90]	[0.70; 1]	[0.50; 0.96]
	Se/Sp (%)	100/60.6	80/70.6	100/47.8	37.5/91.3	100/82.4	60/84.2
TH3	Optimal cut-off	0.048	2.22	65.1	0.45	1.64	3.46
	AUC	0.6	0.61	0.51	0.51	0.51	0.55
	[95% CI]	[0.39; 0.81]	[0.33; 0.89]	[0.30; 0.73]	[0.27; 0.75]	[0.27; 0.75]	[0.31; 0.79]
	Se/Sp (%)	100/68.8	50/75	50/68.7	37.5/78.1	83.3/46.4	83.3/51.7
Rewarm	Optimal cut-off	0.013	2.51	69.6	0.38	1.69	3.88
	AUC	0.58	**0.78***	**0.79*****	**0.77****	0.68	0.56
	[95% CI]	[0.39; 0.77]	[0.57; 0.99]	[0.63; 0.96]	[0.61; 0.94]	[0.48; 0.88]	[0.19; 0.94]
	Se/Sp (%)	75/56.2	100/61.9	85.7/80	85.7/68	100/61.9	66.7/68.2
Post-TH	Optimal cut-off	0.032	2.78	66.9	0.37	1.98	5.60
	AUC	0.61	**0.89*****	0.69	**0.72***	0.59	0.67
	[95% CI]	[0.41; 0.81]	[0.77; 1]	[0.49; 0.9]	[0.51; 0.92]	[0.31; 0.86]	[0.38; 0.96]
	Se/Sp (%)	87.5/36.7	100/74.1	88.9/66.7	88.9/70	80/51.9	60/86.7
Periods	**Predictive variables**	**EEG disc x CRO_2**	**EEG disc x SO_2**	**EEG disc x OEF**	**EEG disc x $CMRO_{2i}$**	**EEG disc x CDO_{2i}**	
TH2	AUC	**0.82****	**0.71***	**0.73***	**0.93*****	**0.90*****	
	[95% CI]	[0.63; 1]	[0.53; 0.89]	[0.55; 0.93]	[0.81; 1]	[0.77; 1]	
	Se/Sp (%)	80/76.5	100/56.5	100/47.8	100/88.2	100/78.9	
TH3	AUC	**0.79***	0.65	0.63	0.6	**0.72***	
	[95% CI]	[0.59; 0.98]	[0.46; 0.84]	[0.43; 0.84]	[0.38; 0.82]	[0.51; 0.94]	
	Se/Sp (%)	80/74.1	100/45.2	100/35.5	100/37	60/85.7	
Rewarm	AUC	**0.83***	**0.77****	**0.78****	0.78	**0.81***	
	[95% CI]	[0.55; 1]	[0.61; 0.94]	[0.62; 0.94]	[0.49; 1]	[0.57; 1]	
	Se/Sp (%)	100/65	100/62.5	100/62.5	100/60	100/66.7	
Post-TH	AUC	**0.9*****	0.67	0.7	**0.76***	**0.92*****	
	[95% CI]	[0.78; 1]	[0.45; 0.89]	[0.48; 0.92]	[0.56; 0.96]	[0.8; 1]	
	Se/Sp (%)	100/76	75/64.3	62.5/82.1	75/80	100/77.8	

Table 3. EEG discontinuity index and FDNIRS-DCS parameters used separately and combined as predictors of normal-mild *vs.* moderate outcomes during therapeutic hypothermia day 2 (TH2), day 3 (TH3), rewarming (Rewarm) and post-therapy (Post-TH). Receiver operating characteristics (ROC) curve (AUC) analysis is presented with optimal cut-off, sensitivity, specificity, and the corresponding 95% confidence interval. *$p < 0.05$; **$p < 0.01$; ***$p < 0.001$. *FDNIRS-DCS:* frequency domain near infrared spectroscopy and diffuse correlation spectroscopy, *EEG:* electroencephalography, *TH:* therapeutic hypothermia, *TH2:* 42-48 h of age, *TH3:* last 6 h of TH, *Rewarm:* 0-6 h post-TH, *Post-TH:* 6-12 h post-TH, *Se:* sensitivity, *Sp:* specificity, *CI:* confidence interval, *EEG disc:* EEG discontinuity index, *CRO_2*: cerebral oxygen reserve, *SO_2*: cerebral oxygen saturation, *OEF:* cerebral oxygen extraction fraction, *$CMRO_{2i}$*: cerebral metabolic rate of oxygen consumption, *CDO_{2i}*: cerebral oxygen delivery.

reports the combined utility of quantitative EEG and FDNIRS-DCS neuromonitoring for prediction of short-term outcomes.

While MRI findings obtained within the first week of life are predictive of later neurodevelopment outcomes[36,37], a prognostic indicator measured at the bedside and available earlier than the post-TH MRI is relevant for critical care management of HIE neonates undergoing TH. Use of combined conventional NIRS and aEEG neuromonitoring for outcome prediction has already been subject of much investigation. Lemmers et al. showed that $rScO_2$ and aEEG scores combined as early as 12 h after birth could reliably predict neurodevelopment outcome at 18 months with higher accuracy than either modality alone[21]. Goeral et al. found that $rScO_2$ alone did not differentiate neonates with or without brain injury on MRI but the combined use of $rScO_2$ with aEEG improved prognostication significantly[25]. In our study, we also showed the added value of combining EEG with FDNIRS-DCS neuromonitoring to predict short-term outcome and its severity.

Several previous studies demonstrated that the predictive value of an EEG/aEEG background at 6 h of age was suboptimal and became more reliable after 24 h[17–19,38]. However, Niezen et al. found that aEEG was a strong predictor of adverse outcome during the entire cooling period (at 6, 12, 24, 48, and 72 h of cooling) and 24 h after rewarming[20]. Also, neonates with abnormal MRI had a higher percentage of abnormal aEEG background patterns than neonates with normal MRI[25]. Excessive EEG discontinuity at 24 h and 48 h and high seizure burden were associated with brain injury on MRI and predictive of abnormal 24-month neurodevelopment outcome[39]. In the current study, EEG discontinuity index was higher in the severe compared to moderate and

normal-mild outcome groups as early as during day 1 and day 2 of TH. However, EEG discontinuity index alone did not demonstrate a significant predictive ability in discriminating between normal-mild and moderate short-term outcomes.

HIE is associated with multiple pathological mechanisms including cortical energy failure, excitotoxicity, neuronal apoptosis, and disruptions in neurotransmitter systems, all of which contribute to the suppression of continuous EEG activity[40–42]. Specific brain regions such as the thalamus, basal ganglia, and cortex are particularly vulnerable to hypoxic-ischemic damage and contribute to the discontinuous EEG patterns observed in these neonates[43–45]. In our study, the association of higher EEG discontinuity index with severe outcomes aligns with findings from prior research[39,46–48]. Importantly, TH can partially restore EEG continuity over time, reflecting improvements in metabolic stability and neuronal function[27,49,50]. These mechanistic insights highlight the value of EEG discontinuity as a biomarker for injury severity and recovery, complementing the metabolic information provided by FDNIRS-DCS.

Several studies have assessed the ability of NIRS neuromonitoring (without DCS) to predict outcomes in HIE neonates with a focus on $rScO_2$ and cFTOE. During TH and rewarming, higher $rScO_2$ measured by continuous-wave[19,51,52] and time-resolved NIRS[53] predicted brain injury on MRI. However, other studies based on continuous-wave NIRS showed that $rScO_2$ during day 3 of TH and rewarming did not consistently predict short-term outcomes[20,23]. Continuous-wave NIRS cFTOE was lower in neonates with adverse compared to favorable neurodevelopmental outcomes[21]. Additionally, Shetty et al. reported lower MRI oxygen extraction fraction after 24 h of life in neonates with severe compared to those with moderate encephalopathy[54]. Our results are consistent with most of these studies showing higher SO_2 and lower OEF during all periods in neonates with severe compared to those with normal-mild outcomes. During certain periods, this pattern was also observed in neonates with severe outcomes compared to those with moderate outcomes.

While TH itself could play a role in reducing brain metabolism[10,34], it might not be the only factor explaining the reduced cerebral oxygen utilization (increased SO_2 and CRO_2 with decreased OEF) in severe compared to normal-mild and moderate outcome groups. The protective "autoregulatory" mechanisms of the brain tightly regulate the rate of oxygen delivery and consumption under healthy conditions to maintain coupling despite changes in temperature and arterial blood pressure[55–57]. However, neonates with HIE undergoing TH may be more susceptible to flow-consumption coupling dysfunction due to the initial hypoxic-ischemic injury and subsequent failure to compensate for vasodilation. This cascade may result in energy failure and further brain injury[58]. In our study, CDO_{2i} and $CMRO_{2i}$ separately did not provide evidences of coupling dysfunction that were statistically significant. On the other hand, CRO_2 which was calculated as the ratio between CDO_{2i} and $CMRO_{2i}$ brought specific information regarding the coupling between CDO_{2i} and $CMRO_{2i}$[59,60]. The higher CRO_2 in severe outcome group compared to moderate and normal-mild outcome groups reflects a higher availability of cerebral oxygen. This higher CRO_2 could potentially be a result of mitochondrial dysfunction that is often triggered by HIE and results in neuronal apoptosis and consequently a decrease in the utilization of oxygen by dead tissues. It is also possible that mitochondrial dysfunction in brain regions with otherwise high metabolism (such as deep gray matter structures) may have led to higher cerebral oxygen supply despite reduced oxygen utilization, known as cerebral hyperperfusion[10,11,15,51,61]. While published literature is sparse on reporting CRO_2[59,60], this parameter allowed to differentiate patients with severe, moderate and normal-mild outcomes and its predictive ability was good. Monitoring CRO_2 using bedside FDNIRS-DCS could provide information on hemodynamic changes potentially leading to flow-consumption coupling dysfunction in term neonates with HIE.

During rewarming, CDO_{2i} showed good predictive ability in discriminating severe from moderate and normal-mild outcome groups. A trend towards increased CDO_{2i} was noticed in the severe group, which could be attributed to the delayed occurrence of cerebral hyperperfusion on day 2–3 due to TH[10,12]. Monitoring CDO_{2i} over the course of rewarming may be useful for identifying neonates with poor tolerance to rewarming due to the inability to adjust to changes in hemodynamics, pressure and temperature during the secondary phase of brain injury[62,63].

Prognostication of moderate brain injury is challenging. Although EEG discontinuity index was not able to differentiate moderate vs. normal-mild outcome patients, $CMRO_{2i}$ was successful as early as day 2 of TH as was CRO_2 later in the post-TH period. The moderate group also presented lower $CMRO_{2i}$ compared to the normal-mild group. This is consistent with reduced $CMRO_{2i}$ observed after hypoxia ischemia in the neonatal lamb[64] as well as in piglets after longer duration of ischemia[65]. These animal studies have shown that $CMRO_{2i}$ could detect insult severity by 8 h after the insult[65]. Therefore, it might be helpful to complement clinical practice with FDNIRS-DCS neuromonitoring in HIE neonates as an early marker of insult severity in moderate cases. How these parameters correlate with long-term neurodevelopmental outcomes should be further investigated.

Our study has several limitations. Sample sizes were modest and unequal between outcome groups, which limited the use of covariate-adjusted ROC curves. FDNIRS-DCS neuromonitoring on the first day of TH was not available for 87% of the patients due to delays in patient recruitment and technical challenges such as performing simultaneous EEG and FDNIRS-DCS neuromonitoring in this critically ill population. FDNIRS-DCS data can be affected by several factors such as skin pigmentation[32,66,67], forehead hair, ambient light, and motion artifacts. Thus, FDNIRS-DCS measurements were repeated during each period of neuromonitoring to minimize poor quality and unusable data. These factors were well-documented during each measurement session and reviewed to evaluate the performance of our algorithm at rejecting noisy data. Prescription of sedatives or antiseizure medications, and temperature changes may have affected the EEG background[68] and FDNIRS-DCS data[34,69], which could further limit their interpretation. In ventilated patients, a method to correct HGB was not used for estimating $CMRO_{2i}$ and CDO_{2i}[70], which may have been slightly affected by oxygen solubility changes. However, HGB was measured every 6–8 h and averaged over each period, limiting the contribution of changes due to oxygen solubility. Collecting the fraction of inspired oxygen may help account for this factor in future studies.

However, this contribution is likely modest in the context of mild TH as hemoglobin-bound oxygen is the predominant contributor to oxygen transport during TH[71]. FDNIRS-DCS monitoring was performed on the frontoparietal regions while EEG discontinuity was assessed on C3-C4 electrodes due to higher presence of artefacts in frontal electrodes. Previous NIRS-EEG studies have used a similar approach[20,21,25]. While HIE is a global phenomenon, frontoparietal neuromonitoring may not capture the full extent of brain injuries occurring in deep brain structures such as the basal ganglia and thalamus. Also, while most FDNIRS-DCS measurements were performed during EEG monitoring, some were not simultaneous with the EEG monitoring but were acquired within a maximal 5 h window. For pre-discharge FDINRS-DCS sessions, age at measurements was not always consistent between patients as length of hospital stay varied between them.

In conclusion, in neonates undergoing TH for HIE, the ability of combined EEG and FDNIRS-DCS neuromonitoring for short-term outcome prediction was shown to be more accurate than either modality alone. EEG discontinuity index and FDNIRS-DCS parameters showed differences when comparing severe, moderate, and normal-mild short-term outcome groups at certain periods during the hospital stay. These non-invasive neuromonitoring parameters were acquired at the bedside thus avoiding patient transportation during TH. Future studies are needed to assess their associations with long-term neurodevelopmental outcomes.

Methods

Study design and population

Fifty-nine neonates diagnosed with HIE and admitted at the CHU Sainte-Justine University Hospital Center neonatal intensive care unit (NICU) were consecutively recruited from June 2017 to September 2021 in this prospective observational cohort study. This study (#2017-1442) and all methods were approved by the institutional review board of the Comité d'éthique de la recherche at Sainte-Justine University Hospital Center, named by the Quebec Government (#FWA00021692) and acts in accordance with Quebec and Canada laws, and the Code of Federal Regulations in the USA. Written informed consent was obtained from parents/guardians for all patients. Inclusion criteria included neonates born at ≥ 35 weeks gestational age, ≥ 1800 g at birth, and evidence of encephalopathy treated with TH. Exclusion criteria were imminent death, congenital malformations, congenital infections, or inborn errors of metabolism. Seven neonates were subsequently excluded: two following postnatal resuscitation for cardiopulmonary arrest, one with neonatal lupus and congenital heart block, three neonates who did not undergo TH, and one who underwent incomplete TH. The remaining fifty-two neonates (N = 52) were considered for subsequent analyses.

All neonates included underwent moderate whole-body TH. Criteria for TH included severe metabolic acidosis with pH ≤ 7 or base deficit ≥ -16, or milder acidosis with pH between 7.01–7.15 or base deficit between -10 to -15.9, accompanied by Apgar score ≤ 5 or positive-pressure ventilation at 10 min, and a sentinel perinatal event. Moderate whole-body TH was initiated within six hours after birth with target core temperature of 33.5 ± 0.5 °C, continued for 72 h, and followed by gradual rewarming of 0.5 °C per hour over 6 h. Sedation was provided at the discretion of the treating physician. Seizures were treated as per the institutional protocol with phenobarbital as the first-line medication. The modified Sarnat exam for evaluation of encephalopathy severity was performed on admission[72–74].

Data collection

Perinatal and neonatal characteristics were retrieved from medical charts. Peripheral oxygen saturation (SpO_2, %) was measured from preductal pulse oximetry at an upper limb. Then the average of SpO_2 values before and after FDNIRS-DCS neuromonitoring were averaged and used further. Blood was collected every 6–8 h during TH and less frequently following MRI. Hemoglobin concentrations (HGB, g/dl) were obtained using hematological analysis throughout the hospital stay and extracted from medical records.

EEG recording and quantitative analysis of EEG discontinuity

Video-EEG was recorded using portable Stellate Vita ICU (Natus Medical, Ottawa, ON, Canada) or Nihon Kohden video-EEG systems (Nihon Kohden America, Irvine, CA, USA) and acquired with a 200 Hz sampling rate and 0.1–100 Hz bandpass. Certified EEG technologists applied surface electrodes according to the international 10–20 system of electrodes placement modified for neonates (Fp1, Fp2, T3, T4, C3, C4, Cz, Fz, Pz, O1, and O2). All neonates underwent continuous EEG monitoring as soon as possible during TH and for at least 6 h post-rewarming.

Quantitative calculation of an index of EEG discontinuity was performed using BrainVision software (Brain Products, GmbH, Germany) and recordings were digitally filtered (0.5–50 Hz bandpass, 60 Hz notch) and re-sampled at 256 Hz to ensure minimal residual aliasing artifacts[75]. EEG segments containing artefacts were rejected after the use of the automatic artifact rejection from BrainVision software. Following this procedure, a visual inspection was performed to remove residual artifacts. The following 6-h epochs were considered: 18-24 h of age (TH1), 42-48 h of age (TH2), last 6 h of TH (TH3), 0-6 h post-TH (Rewarm), and 6-12 h post-TH (Post-TH). The quantification of EEG discontinuity was previously described by our group[68,76]. A minimum of 60 min of artefact-free recording per 6 h epoch was required for inclusion in the analysis. Consequently, the number of recordings included per period were 48, 52, 50, 50, and 48, respectively. Epochs were partitioned into non-overlapping consecutive temporal segments of 2 s. An EEG discontinuity index was calculated as the proportion of low voltage segments with a peak-to-peak amplitude < 15 μV within a given 6-h epoch. EEG data derived from the central pair of electrodes (C3-C4) were retained for analyses, as these channels were less susceptible to artefacts[77]. A threshold of < 15 μV was selected to avoid the inclusion of the normal discontinuous *tracé alternant* background pattern, with activity typically ≥ 25 μV interrupted by medium–high voltage fast waveforms that is physiologically present during quiet sleep in healthy neonates. Normal background activity in term neonates has peak-to-peak amplitudes above 25 μV in all behavioral states[78,79].

Non-invasive bedside optical neuromonitoring

FDNIRS-DCS neuromonitoring was performed with a commercial system (MetaOx, ISS Inc., Champaign, IL, USA)[30,31]. The system was approved by Health Canada for research purpose only. The optical sensor was designed and developed to image the neonatal cortex[80]. For FDNIRS, the source-detector distances were 10, 15, 20, and 25 mm while 8 co-located DCS optical fibers were positioned at 22 mm from the source. This optical configuration was used to minimize signal contamination due to head curvature[80]. Optical energy exposure satisfied the American National Standards Institute (ANSI) standard for Safe Use of Lasers and related regulations[81].

The sensor was delicately positioned on the middle frontal location as well as left and right frontoparietal locations of the head and signals were recorded 5 times in each location by repositioning the sensor slightly to account for local inhomogeneities. Analysis was performed offline. Data quality assessment and data rejection were performed with published criteria[34,82–88] prior to averaging data from the three locations per session.

FDNIRS-DCS neuromonitoring was performed throughout the hospitalization of the neonate, starting from day 2 of TH. Each measurement session required ~ 20 min. During day 2 of TH (25 h-48 h of age, TH2) and day 3 of TH (49 h-72 h of age, TH3) periods, measurements were performed twice daily. During rewarming (0-6 h post-TH, Rewarm) and post-therapy (6-12 h post-TH, Post-TH), at least 2 measurements per period were performed, followed by one measurement before hospital discharge when patients were normothermic (last 2 days before discharge, Pre-DC). These measurements were further grouped and averaged into these five non-overlapping periods. The number of measurements that satisfied data quality and rejection criteria per period were 51, 88, 69, 93 and 77, respectively.

Using FDNIRS signals, SO_2 (%) was derived and calculated by the ratio between oxyhemoglobin (HbO_2, µmol/L) and total hemoglobin ($HbT = HbO_2 + HbR$) concentrations, where HbR is the deoxyhemoglobin concentration. $CMRO_{2i}$ (mL O_2/dL × mm^2/s) was derived via the Fick's principle[82] as in previous studies[34,83–86,88,89] and calculated by the product of arterial oxygen concentration (CaO_2, mL O_2/dL of blood), the portion of cardiac output distributed to the brain, which was estimated by CBF_i (mm^2/s) and derived from DCS signals[32,33], and OEF. Arterial oxygen concentration was derived such that $CaO_2 = \gamma \times HGB \times SpO_2$, where $\gamma = 1.39$ (mL O_2/g of HGB) is the theoretical maximum oxygen carrying capacity. Cerebral OEF was defined by the ratio between the arterio-venous O_2 saturation difference (SpO_2–SvO_2) and SpO_2. SvO_2 was derived from a weighted sum of SpO_2 and absolute SO_2 such that $SO_2 = \alpha SpO_2 + \beta SvO_2$, with $\alpha + \beta = 1$, assuming the arterial:venous compartment ratio is 0.25:0.75[90]. The following formula was used to derive CDO_{2i} (mL O_2/dL × mm^2/s): $CDO_{2i} = \gamma \times CBF_i \times HGB \times SpO_2$. To calculate CRO_2, the ratio between CDO_{2i} and $CMRO_{2i}$ was applied. The calculation of these parameters was performed in MATLAB (Mathworks, Natick, MA, USA) version R2018b.

Short-term outcome

After rewarming, clinical MRI was performed on a 1.5 T or 3 T MRI scanner at a median age of 5 days (interquartile range [IQR] 4–6). MRI sequences included sagittal and axial T1-weighted imaging and T2-weighted imaging, diffusion-weighted imaging (DWI), and susceptibility-weighted imaging. A pediatric radiologist blinded to the clinical characteristics of the study cohort reviewed the MRI scans. The severity, type and location of brain injury was evaluated in the following brain regions: cerebral hemispheres, basal ganglia and thalamus (BGT), anterior (ALIC) and posterior (PLIC) limb of the internal capsule, cerebellum, and corona radiata[91,92]. Areas of watershed infarction (focal or territorial), size of cerebral lesions (minimal or extensive), venous sinus thrombosis, and hemorrhage staging (acute, subacute, chronic or late chronic) were also documented[91,92]. Based on MRI injury pattern, neonates were subsequently classified into the following short-term outcome groups: normal-mild (normal or minimal cerebral lesions with no areas of watershed infarction and no involvement of BGT, PLIC or ALIC), moderate (any PLIC or ALIC or area of watershed or focal infarction, with no involvement of BGT), or severe (involvement of BGT, or global hypoxic-ischemic injury pattern, or death prior to discharge)[91].

Statistical analysis

The three short-term outcome groups (normal-mild, moderate and severe) were compared. Considering the different samples sizes in these three groups and non-normal data distribution, non-parametric tests were performed. Demographics and data were expressed using standard descriptive statistics with continuous variables presented with median and IQR, and categorical variables presented in frequency and percentage. To determine if there were differences in demographics and clinical variables between the three outcome groups, Kruskal–Wallis tests followed by post-hoc comparison using Mann–Whitney U tests were performed for continuous variables and chi-square tests for categorical variables. This approach was also used to assess differences in EEG discontinuity and FDNIRS-DCS parameters between outcome groups. Comparisons were corrected for multiplicity using the Benjamini–Hochberg procedure[93] and considered significant at $p < 0.05$.

Non-parametric area under the ROC curve analysis[94–96] was performed to assess which EEG discontinuity and FDNIRS-DCS parameters were associated with the short-term outcomes. These analyses considered data skewness. For each monitoring period (TH2, TH3, Rewarm and Post-TH), the following statistical models were assessed 1) moderate *vs.* severe outcomes, 2) normal-mild *vs.* moderate outcomes, and 3) normal-mild vs. severe outcomes. To test the interaction between EEG and FDNIRS-DCS, the prognostic ability was assessed by multiplying EEG discontinuity index with each FDNIRS-DCS parameter[21,25]. Binary logistic regression analysis was used first to obtain the predictive probabilities for each combination, then AUC analysis was performed. ROC curves were used to detect the optimal cut-off points (only for single parameter models) and for calculation of sensitivity and specificity. An AUC score ≥ 0.8 was considered good predictive accuracy[95]. AUC scores and corresponding 95% confident intervals were also reported. Statistical analyses were performed using IBM SPSS Statistics for Windows, version 27.0 (IBM Corp., Armonk, N.Y., USA).

Data availability

The raw data supporting the findings of this article will be made available by the corresponding author upon appropriate request.

Received: 9 July 2024; Accepted: 26 May 2025
Published online: 06 June 2025

References

1. Allen, K. A. & Brandon, D. H. Hypoxic Ischemic Encephalopathy: Pathophysiology and Experimental Treatments. *Newborn Infant Nurs. Rev.* **11**, 125–133. https://doi.org/10.1053/j.nainr.2011.07.004 (2011).
2. Schiariti, V. et al. Perinatal characteristics and parents' perspective of health status of NICU graduates born at term. *J. Perinatol.* **28**, 368–376. https://doi.org/10.1038/jp.2008.9 (2008).
3. Ferriero, D. M. Neonatal brain injury. *N. Engl. J. Med.* **351**, 1985–1995. https://doi.org/10.1056/NEJMra041996 (2004).
4. Lawn, J., Shibuya, K. & Stein, C. No cry at birth: global estimates of intrapartum stillbirths and intrapartum-related neonatal deaths. *Bull. World Health Organ.* **83**, 409–417 (2005).
5. Jacobs, S. E. et al. Whole-body hypothermia for term and near-term newborns with hypoxic-ischemic encephalopathy: a randomized controlled trial. *Arch. Pediatr. Adolesc Med.* **165**, 692–700. https://doi.org/10.1001/archpediatrics.2011.43 (2011).
6. Shankaran, S. et al. Evolution of encephalopathy during whole body hypothermia for neonatal hypoxic-ischemic encephalopathy. *J. Pediatr.* **160**, 567-572 e563. https://doi.org/10.1016/j.jpeds.2011.09.018 (2012).
7. Tagin, M. A., Woolcott, C. G., Vincer, M. J., Whyte, R. K. & Stinson, D. A. Hypothermia for neonatal hypoxic ischemic encephalopathy: an updated systematic review and meta-analysis. *Arch. Pediatr. Adolesc. Med.* **166**, 558–566. https://doi.org/10.1001/archpediatrics.2011.1772 (2012).
8. Jacobs, S. E. et al. Cooling for newborns with hypoxic ischaemic encephalopathy. *Cochrane Database Syst. Rev.* https://doi.org/10.1002/14651858.CD003311.pub3 (2013).
9. Greisen, G. Cerebral blood flow and oxygenation in infants after birth asphyxia. Clinically useful information?. *Early Hum. Dev.* **90**, 703–705. https://doi.org/10.1016/j.earlhumdev.2014.06.007 (2014).
10. Wintermark, P. et al. Brain perfusion in asphyxiated newborns treated with therapeutic hypothermia. *AJNR Am. J. Neuroradiol.* **32**, 2023–2029. https://doi.org/10.3174/ajnr.A2708 (2011).
11. Kleuskens, D. G. et al. Pathophysiology of cerebral hyperperfusion in term neonates with hypoxic-ischemic encephalopathy: A systematic review for future research. *Front. Pediatr.* **9**, 631258. https://doi.org/10.3389/fped.2021.631258 (2021).
12. Chakkarapani, E. et al. Effects of xenon and hypothermia on cerebrovascular pressure reactivity in newborn global hypoxic-ischemic pig model. *J. Cereb. Blood Flow Metab.* **33**, 1752–1760. https://doi.org/10.1038/jcbfm.2013.123 (2013).
13. Dhillon, S. K. et al. Cerebral oxygenation and metabolism after hypoxia-ischemia. *Front. Pediatr.* **10**, 925951. https://doi.org/10.3389/fped.2022.925951 (2022).
14. Wassink, G. et al. Therapeutic hypothermia in neonatal hypoxic-ischemic encephalopathy. *Curr. Neurol. Neurosci. Rep.* **19**, 2. https://doi.org/10.1007/s11910-019-0916-0 (2019).
15. Wintermark, P., Hansen, A., Warfield, S. K., Dukhovny, D. & Soul, J. S. Near-infrared spectroscopy versus magnetic resonance imaging to study brain perfusion in newborns with hypoxic–ischemic encephalopathy treated with hypothermia. *Neuroimage* **85**, 287–293. https://doi.org/10.1016/j.neuroimage.2013.04.072 (2014).
16. Thorngren-Jerneck, K., Hellstrom-Westas, L., Ryding, E. & Rosen, I. Cerebral glucose metabolism and early EEG/aEEG in term newborn infants with hypoxic-ischemic encephalopathy. *Pediatr Res.* **54**, 854–860. https://doi.org/10.1203/01.PDR.0000088068.82225.96 (2003).
17. Thoresen, M., Hellstrom-Westas, L., Liu, X. & de Vries, L. S. Effect of hypothermia on amplitude-integrated electroencephalogram in infants with asphyxia. *Pediatrics* **126**, e131-139. https://doi.org/10.1542/peds.2009-2938 (2010).
18. Chandrasekaran, M., Chaban, B., Montaldo, P. & Thayyil, S. Predictive value of amplitude-integrated EEG (aEEG) after rescue hypothermic neuroprotection for hypoxic ischemic encephalopathy: a meta-analysis. *J. Perinatol.* **37**, 684–689. https://doi.org/10.1038/jp.2017.14 (2017).
19. Ancora, G. et al. Early predictors of short term neurodevelopmental outcome in asphyxiated cooled infants. A combined brain amplitude integrated electroencephalography and near infrared spectroscopy study. *Brain Dev.* **35**, 26–31. https://doi.org/10.1016/j.braindev.2011.09.008 (2013).
20. Niezen, C. K., Bos, A. F., Sival, D. A., Meiners, L. C. & Ter Horst, H. J. Amplitude-integrated EEG and cerebral near-infrared spectroscopy in cooled asphyxiated infants. *Am. J. Perinatol.* **35**, 904–910. https://doi.org/10.1055/s-0038-1626712 (2018).
21. Lemmers, P. M. et al. Cerebral oxygenation and brain activity after perinatal asphyxia: does hypothermia change their prognostic value?. *Pediatr. Res.* **74**, 180–185. https://doi.org/10.1038/pr.2013.84 (2013).
22. Jain, S. V. et al. Cerebral regional oxygen saturation trends in infants with hypoxic-ischemic encephalopathy. *Early Hum. Dev.* **113**, 55–61. https://doi.org/10.1016/j.earlhumdev.2017.07.008 (2017).
23. Shellhaas, R. A. et al. Limited short-term prognostic utility of cerebral NIRS during neonatal therapeutic hypothermia. *Neurology* **81**, 249–255. https://doi.org/10.1212/WNL.0b013e31829bfe41 (2013).
24. Variane, G. F. T., Chock, V. Y., Netto, A., Pietrobom, R. F. R. & Van Meurs, K. P. Simultaneous near-infrared spectroscopy (NIRS) and amplitude-integrated electroencephalography (aEEG): Dual use of brain monitoring techniques improves our understanding of physiology. *Front. Pediatr.* **7**, 560. https://doi.org/10.3389/fped.2019.00560 (2019).
25. Goeral, K. et al. Prediction of outcome in neonates with hypoxic-ischemic encephalopathy II: Role of amplitude-integrated electroencephalography and cerebral oxygen saturation measured by near-infrared spectroscopy. *Neonatology* **112**, 193–202. https://doi.org/10.1159/000468976 (2017).
26. Jain, S. V., Zempel, J. M., Srinivasakumar, P., Wallendorf, M. & Mathur, A. Early EEG power predicts MRI injury in infants with hypoxic-ischemic encephalopathy. *J. Perinatol.* **37**, 541–546. https://doi.org/10.1038/jp.2016.262 (2017).
27. Dereymaeker, A. et al. Automated EEG background analysis to identify neonates with hypoxic-ischemic encephalopathy treated with hypothermia at risk for adverse outcome: A pilot study. *Pediatr. Neonatol.* **60**, 50–58. https://doi.org/10.1016/j.pedneo.2018.03.010 (2019).
28. Grant, P. E. et al. Increased cerebral blood volume and oxygen consumption in neonatal brain injury. *J. Cereb. Blood Flow Metab.* **29**, 1704–1713. https://doi.org/10.1038/jcbfm.2009.90 (2009).
29. Franceschini, M. A. et al. Assessment of infant brain development with frequency-domain near-infrared spectroscopy. *Pediatr. Res.* **61**, 546–551. https://doi.org/10.1203/pdr.0b013e318045be99 (2007).
30. Carp, S. A., Farzam, P., Redes, N., Hueber, D. M. & Franceschini, M. A. Combined multi-distance frequency domain and diffuse correlation spectroscopy system with simultaneous data acquisition and real-time analysis. *Biomed. Opt. Express* **8**, 3993–4006. https://doi.org/10.1364/BOE.8.003993 (2017).
31. Buckley, E. M. et al. A Novel Combined Frequency-Domain Near-Infrared Spectroscopy and Diffuse Correlation Spectroscopy System. In *Biomedical Optics 2014*, OSA Technical Digest (online) (Optica Publishing Group, 2014), paper BM3A.17.

32. Cheung, C., Culver, J. P., Takahashi, K., Greenberg, J. H. & Yodh, A. G. In vivo cerebrovascular measurement combining diffuse near-infrared absorption and correlation spectroscopies. *Phys. Med. Biol.* **46**, 2053–2065. https://doi.org/10.1088/0031-9155/46/8/302 (2001).
33. Boas, D. A. & Yodh, A. G. Spatially varying dynamical properties of turbid media probed with diffusing temporal light correlation. *J. Opt. Soc. Am. Opt. Image Sci. Vis.* **14**, 192–215 (1997).
34. Dehaes, M. et al. Cerebral oxygen metabolism in neonatal hypoxic ischemic encephalopathy during and after therapeutic hypothermia. *J. Cereb. Blood Flow Metab.* **34**, 87–94. https://doi.org/10.1038/jcbfm.2013.165 (2014).
35. Nevalainen, P. et al. Evoked potentials recorded during routine EEG predict outcome after perinatal asphyxia. *Clin. Neurophysiol.* **128**, 1337–1343. https://doi.org/10.1016/j.clinph.2017.04.025 (2017).
36. O'Kane, A. et al. Early versus late brain magnetic resonance imaging after neonatal hypoxic ischemic encephalopathy treated with therapeutic hypothermia. *J. Pediatr.* **232**, 73-79.e72. https://doi.org/10.1016/j.jpeds.2021.01.050 (2021).
37. Bach, A. M. et al. Early magnetic resonance imaging predicts 30-month outcomes after therapeutic hypothermia for neonatal encephalopathy. *J. Pediatr.* **238**, 94-101.e1. https://doi.org/10.1016/j.jpeds.2021.07.003 (2021).
38. Ouwehand, S. et al. Predictors of outcomes in hypoxic-ischemic encephalopathy following hypothermia: A meta-analysis. *Neonatology* **117**, 411–427. https://doi.org/10.1159/000505519 (2020).
39. Dunne, J. M. et al. Automated electroencephalographic discontinuity in cooled newborns predicts cerebral MRI and neurodevelopmental outcome. *Arch. Dis. Child Fetal Neonatal Ed.* **102**, F58–F64. https://doi.org/10.1136/archdischild-2015-309697 (2017).
40. Ching, S., Purdon, P. L., Vijayan, S., Kopell, N. J. & Brown, E. N. A neurophysiological-metabolic model for burst suppression. *Proc. Natl. Acad. Sci. USA* **109**, 3095–3100. https://doi.org/10.1073/pnas.1121461109 (2012).
41. Niedermeyer, E., Sherman, D. L., Geocadin, R. J., Hansen, H. C. & Hanley, D. F. The burst-suppression electroencephalogram. *Clin. Electroencephalogr.* **30**, 99–105. https://doi.org/10.1177/155005949903000305 (1999).
42. Roberts, J. A., Iyer, K. K., Finnigan, S., Vanhatalo, S. & Breakspear, M. Scale-free bursting in human cortex following hypoxia at birth. *J. Neurosci.* **34**, 6557–6572. https://doi.org/10.1523/JNEUROSCI.4701-13.2014 (2014).
43. Kebaya, L. M. N. et al. Subcortical brain volumes in neonatal hypoxic–ischemic encephalopathy. *Pediatr. Res.* **94**, 1797–1803. https://doi.org/10.1038/s41390-023-02695-y (2023).
44. Chalia, M. et al. Hemodynamic response to burst-suppressed and discontinuous electroencephalography activity in infants with hypoxic ischemic encephalopathy. *Neurophotonics* **3**, 031408. https://doi.org/10.1117/1.NPh.3.3.031408 (2016).
45. Gloor, P. Neuronal generators and the problem of localization in electroencephalography: application of volume conductor theory to electroencephalography. *J. Clin. Neurophysiol.* **2**, 327–354. https://doi.org/10.1097/00004691-198510000-00002 (1985).
46. van Rooij, L. G. et al. Recovery of amplitude integrated electroencephalographic background patterns within 24 hours of perinatal asphyxia. *Arch. Dis. Child Fetal Neonatal Ed.* **90**, F245-251. https://doi.org/10.1136/adc.2004.064964 (2005).
47. Menache, C. C., Bourgeois, B. F. & Volpe, J. J. Prognostic value of neonatal discontinuous EEG. *Pediatr. Neurol.* **27**, 93–101 (2002).
48. Awal, M. A., Lai, M. M., Azemi, G., Boashash, B. & Colditz, P. B. EEG background features that predict outcome in term neonates with hypoxic ischaemic encephalopathy: A structured review. *Clin. Neurophysiol.* **127**, 285–296. https://doi.org/10.1016/j.clinph.2015.05.018 (2016).
49. Douglas-Escobar, M. & Weiss, M. D. Hypoxic-ischemic encephalopathy: a review for the clinician. *JAMA Pediatr.* **169**, 397–403. https://doi.org/10.1001/jamapediatrics.2014.3269 (2015).
50. Gunn, A. J. & Thoresen, M. Neonatal encephalopathy and hypoxic-ischemic encephalopathy. *Handb. Clin. Neurol.* **162**, 217–237. https://doi.org/10.1016/B978-0-444-64029-1.00010-2 (2019).
51. Peng, S. et al. Does near-infrared spectroscopy identify asphyxiated newborns at risk of developing brain injury during hypothermia treatment?. *Am. J. Perinatol.* **32**, 555–564. https://doi.org/10.1055/s-0034-1396692 (2015).
52. Szakmar, E. et al. Association between cerebral oxygen saturation and brain injury in neonates receiving therapeutic hypothermia for neonatal encephalopathy. *J. Perinatol.* **41**, 269–277. https://doi.org/10.1038/s41372-020-00910-w (2021).
53. Nakamura, S. et al. Simultaneous measurement of cerebral hemoglobin oxygen saturation and blood volume in asphyxiated neonates by near-infrared time-resolved spectroscopy. *Brain Dev.* **37**, 925–932. https://doi.org/10.1016/j.braindev.2015.04.002 (2015).
54. Shetty, A. N. et al. Cerebral oxygen metabolism during and after therapeutic hypothermia in neonatal hypoxic-ischemic encephalopathy: a feasibility study using magnetic resonance imaging. *Pediatr. Radiol.* **49**, 224–233. https://doi.org/10.1007/s00247-018-4283-9 (2019).
55. Rhee, C. J. et al. Neonatal cerebrovascular autoregulation. *Pediatr. Res.* **84**, 602–610. https://doi.org/10.1038/s41390-018-0141-6 (2018).
56. Wu, T. W., Tamrazi, B., Soleymani, S., Seri, I. & Noori, S. Hemodynamic changes during rewarming phase of whole-body hypothermia therapy in neonates with hypoxic-ischemic encephalopathy. *J. Pediatr.* **197**, 68-74.e62. https://doi.org/10.1016/j.jpeds.2018.01.067 (2018).
57. Bakhsheshi, M. F., Diop, M., Morrison, L. B., St Lawrence, K. & Lee, T. Y. Coupling of cerebral blood flow and oxygen consumption during hypothermia in newborn piglets as measured by time-resolved near-infrared spectroscopy: a pilot study. *Neurophotonics* **2**, 035006 (2015).
58. Powers, W. J., Grubb, R. L. Jr., Darriet, D. & Raichle, M. E. Cerebral blood flow and cerebral metabolic rate of oxygen requirements for cerebral function and viability in humans. *J. Cereb. Blood Flow Metab.* **5**, 600–608. https://doi.org/10.1038/jcbfm.1985.89 (1985).
59. Goenarjo, R. et al. Cerebral oxygenation reserve: The relationship between physical activity level and the cognitive load during a stroop task in healthy young males. *Int. J. Environ. Res. Public Health* https://doi.org/10.3390/ijerph17041406 (2020).
60. Spinelli, E. & Bartlett, R. H. Anemia and transfusion in critical care: Physiology and management. *J. Intens. Care Med.* **31**, 295–306. https://doi.org/10.1177/0885066615571901 (2016).
61. Proisy, M. et al. Changes in brain perfusion in successive arterial spin labeling MRI scans in neonates with hypoxic-ischemic encephalopathy. *Neuroimage Clin.* **24**, 101939. https://doi.org/10.1016/j.nicl.2019.101939 (2019).
62. Gebauer, C. M., Knuepfer, M., Robel-Tillig, E., Pulzer, F. & Vogtmann, C. Hemodynamics among neonates with hypoxic-ischemic encephalopathy during whole-body hypothermia and passive rewarming. *Pediatrics* **117**, 843–850. https://doi.org/10.1542/peds.2004-1587 (2006).
63. Chalak, L. F. et al. Association between increased seizures during rewarming after hypothermia for neonatal hypoxic ischemic encephalopathy and abnormal neurodevelopmental outcomes at 2-year follow-up: A nested multisite cohort study. *JAMA Neurol.* **78**, 1484–1493. https://doi.org/10.1001/jamaneurol.2021.3723 (2021).
64. Rosenberg, A. A. Cerebral blood flow and O_2 metabolism after asphyxia in neonatal lambs. *Pediatr. Res.* **20**, 778–782. https://doi.org/10.1203/00006450-198608000-00016 (1986).
65. Tichauer, K. M. et al. Assessing the severity of perinatal hypoxia-ischemia in piglets using near-infrared spectroscopy to measure the cerebral metabolic rate of oxygen. *Pediatr. Res.* **65**, 301–306. https://doi.org/10.1203/PDR.0b013e318194faa6 (2009).
66. Wassenaar, E. B. & Van den Brand, J. G. Reliability of near-infrared spectroscopy in people with dark skin pigmentation. *J. Clin. Monit. Comput.* **19**, 195–199. https://doi.org/10.1007/s10877-005-1655-0 (2005).
67. Matas, A., Sowa, M. G., Taylor, G. & Mantsch, H. H. Melanin as a confounding factor in near infrared spectroscopy of skin. *Vib. Spectrosc.* **28**, 45–52. https://doi.org/10.1016/S0924-2031(01)00144-8 (2002).

68. Mahdi, Z. et al. Opioid analgesia and temperature regulation are associated with EEG background activity and MRI outcomes in neonates with mild-to-moderate hypoxic-ischemic encephalopathy undergoing therapeutic hypothermia. *Eur. J. Paediatr. Neurol.* **39**, 11–18. https://doi.org/10.1016/j.ejpn.2022.04.001 (2022).
69. Rhoney, D. H. & Parker, D. Jr. Use of sedative and analgesic agents in neurotrauma patients: effects on cerebral physiology. *Neurol Res.* **23**, 237–259. https://doi.org/10.1179/016164101101198398 (2001).
70. Benson, E. J. et al. Diffuse optical monitoring of cerebral hemodynamics and oxygen metabolism during and after cardiopulmonary bypass: Hematocrit correction and neurological vulnerability. *Metabolites* https://doi.org/10.3390/metabo13111153 (2023).
71. Ma, H. et al. Therapeutic hypothermia as a neuroprotective strategy in neonatal hypoxic-ischemic brain injury and traumatic brain injury. *Curr. Mol. Med.* **12**, 1282–1296. https://doi.org/10.2174/156652412803833517 (2012).
72. Chawla, S., Bates, S. V. & Shankaran, S. Is it time for a randomized controlled trial of hypothermia for mild hypoxic-ischemic encephalopathy?. *J. Pediatr.* **220**, 241–244. https://doi.org/10.1016/j.jpeds.2019.11.030 (2020).
73. Sarnat, H. B. & Sarnat, M. S. Neonatal encephalopathy following fetal distress. A clinical and electroencephalographic study. *Arch. Neurol.* **33**, 696–705. https://doi.org/10.1001/archneur.1976.00500100030012 (1976).
74. Shankaran, S. et al. Whole-body hypothermia for neonates with hypoxic-ischemic encephalopathy. *N. Engl. J. Med.* **353**, 1574–1584. https://doi.org/10.1056/NEJMcps050929 (2005).
75. Babiloni, C. et al. International federation of clinical neurophysiology (IFCN)—EEG research workgroup: Recommendations on frequency and topographic analysis of resting state EEG rhythms. Part 1: Applications in clinical research studies. *Clin. Neurophysiol.* **131**, 285–307. https://doi.org/10.1016/j.clinph.2019.06.234 (2020).
76. Birca, A. et al. Rewarming affects EEG background in term newborns with hypoxic-ischemic encephalopathy undergoing therapeutic hypothermia. *Clin. Neurophysiol.* **127**, 2087–2094. https://doi.org/10.1016/j.clinph.2015.12.013 (2016).
77. Glass, H. C., Wusthoff, C. J. & Shellhaas, R. A. Amplitude-integrated electro-encephalography: the child neurologist's perspective. *J. Child Neurol.* **28**, 1342–1350. https://doi.org/10.1177/0883073813488663 (2013).
78. Clancy, R. R. et al. Agreement between long-term neonatal background classification by conventional and amplitude-integrated EEG. *J. Clin. Neurophysiol.* **28**, 1–9. https://doi.org/10.1097/WNP.0b013e3182051105 (2011).
79. Tsuchida, T. N. et al. American clinical neurophysiology society standardized EEG terminology and categorization for the description of continuous EEG monitoring in neonates: report of the American clinical neurophysiology society critical care monitoring committee. *J. Clin. Neurophysiol.* **30**, 161–173. https://doi.org/10.1097/WNP.0b013e3182872b24 (2013).
80. Dehaes, M. et al. Assessment of the frequency-domain multi-distance method to evaluate the brain optical properties: Monte Carlo simulations from neonate to adult. *Biomed. Opt. Express* **2**, 552–567. https://doi.org/10.1364/BOE.2.000552 (2011).
81. *American National Standard for Safe Use of Lasers* <https://www.lia.org/resources/laser-safety-information/laser-safety-standards/ansi-z136-standards> (2014).
82. Lin, P. Y. et al. Non-invasive optical measurement of cerebral metabolism and hemodynamics in infants. *J. Vis. Exp.* https://doi.org/10.3791/4379 (2013).
83. Dehaes, M. et al. Perioperative cerebral hemodynamics and oxygen metabolism in neonates with single-ventricle physiology. *Biomed. Opt. Express* **6**, 4749–4767. https://doi.org/10.1364/BOE.6.004749 (2015).
84. Roche-Labarbe, N. et al. Near-infrared spectroscopy assessment of cerebral oxygen metabolism in the developing premature brain. *J. Cereb. Blood Flow Metab.* **32**, 481–488. https://doi.org/10.1038/jcbfm.2011.145 (2012).
85. Lin, P. Y. et al. Regional and hemispheric asymmetries of cerebral hemodynamic and oxygen metabolism in newborns. *Cereb. Cortex* **23**, 339–348. https://doi.org/10.1093/cercor/bhs023 (2013).
86. Charbonneau, L. et al. Fetal cardiac and neonatal cerebral hemodynamics and oxygen metabolism in transposition of the great arteries. *Ultrasound Obstet. Gynecol.* **61**, 346–355. https://doi.org/10.1002/uog.26146 (2023).
87. Roche-Labarbe, N. et al. Noninvasive optical measures of CBV, StO(2), CBF index, and rCMRO(2) in human premature neonates' brains in the first six weeks of life. *Hum. Brain Mapp.* **31**, 341–352. https://doi.org/10.1002/hbm.20868 (2010).
88. Cote-Corriveau, G. et al. Associations between neurological examination at term-equivalent age and cerebral hemodynamics and oxygen metabolism in infants born preterm. *Front. Neurosci.* **17**, 1105638. https://doi.org/10.3389/fnins.2023.1105638 (2023).
89. Kety, S. S. & Schmidt, C. F. The nitrous oxide method for the quantitative determination of cerebral blood flow in man: theory, procedure and normal values. *J. Clin. Invest.* **27**, 476–483. https://doi.org/10.1172/JCI101994 (1948).
90. Watzman, H. M. et al. Arterial and venous contributions to near-infrared cerebral oximetry. *Anesthesiology* **93**, 947–953 (2000).
91. Shankaran, S. et al. Brain injury following trial of hypothermia for neonatal hypoxic-ischaemic encephalopathy. *Arch. Dis. Child Fetal Neonatal Ed.* **97**, F398-404. https://doi.org/10.1136/archdischild-2011-301524 (2012).
92. Bhagat, I. et al. Does severity of brain injury on magnetic resonance imaging predict short-term outcome in neonates who received therapeutic hypothermia?. *Am. J. Perinatol.* https://doi.org/10.1055/s-0041-1730431 (2021).
93. Benjamini, Y. & Hochberg, Y. Controlling the false discovery rate: A practical and powerful approach to multiple testing. *J. Roy. Stat. Soc.: Ser. B (Methodol.)* **57**, 289–300. https://doi.org/10.1111/j.2517-6161.1995.tb02031.x (2018).
94. Lusted, L. B. Signal detectability and medical decision-making. *Science* **171**, 1217–1219. https://doi.org/10.1126/science.171.3977.1217 (1971).
95. Nahm, F. S. Receiver operating characteristic curve: overview and practical use for clinicians. *Korean J. Anesthesiol.* **75**, 25–36. https://doi.org/10.4097/kja.21209 (2022).
96. Hanley, J. A. & McNeil, B. J. The meaning and use of the area under a receiver operating characteristic (ROC) curve. *Radiology* **143**, 29–36. https://doi.org/10.1148/radiology.143.1.7063747 (1982).
97. Miller, S. P. et al. Seizure-associated brain injury in term newborns with perinatal asphyxia. *Neurology* **58**, 542–548. https://doi.org/10.1212/wnl.58.4.542 (2002).

Acknowledgements

We thank the families who consented to participate in this study, as well as the staff, nurses, technologists, and physicians at CHU Sainte-Justine University Hospital Centre, including colleagues in the departments of Neonatology, Neurology and Radiology. Special thanks to research coordinator Imen Ben Hmida, professional statistician Mi-Suk Kang Dufour, and research nurses Guylaine Aubé, Céline Houssemaine and Karine Fondrouge in addition to all undergraduate, graduate, and medical students who performed bedside FDNIRS-DCS measurements, days and nights over weeks and weekends. The authors would also like to acknowledge funding from the Canadian Institutes of Health Research (CIHR) grant 366072 [to AB and MD, and subsequently to MD and EFP], the Natural Sciences and Engineering Research Council of Canada (NSERC) Discovery grant RGPIN-2015-04672 [to MD], the Fonds de Recherche du Quebec-Santé (FRQS) grant 32600 [to MD] and 311144 [to EFP] as well as financial support from the Sainte-Justine Hospital University Centre Foundation, the TransMedTech Institute and NSERC [to RAC]. This research was conducted as part of the TransMedTech Institute's activities and thanks, in part, to funding from the Canada First Research Excellence Fund. We also want to thank the family that organized a fundraiser for HIE research « Le Relais magique » and all those that participated to improve neuroprotection in newborns with hypoxic-ischemic encephalopathy. This study is dedicated to the memory of our wonderful colleague,

Dr. Ala Birca, who's notable career was devoted to ensuring optimal brain health and neurodevelopment in critically ill neonates.

Author contributions

RAC contributed to the protocol development, methodology, literature review, data curation, acquisition, analysis, statistics, interpretation, drafting of initial manuscript to redaction and revision of the manuscript. ZM contributed to the literature review, methodology, data curation, acquisition, analysis, statistics, interpretation, drafting of initial manuscript, and revision and approval of the manuscript. BD contributed to data curation, acquisition, revision, and approval of the manuscript. BM contributed to the data acquisition, revision, and approval of the manuscript. AB contributed to the conceptualization and design of the study, protocol development, and methodology. REJ contributed to the analysis of MRI data, revision, and approval of the manuscript. AMN contributed to the protocol development, revision, and approval of the manuscript. EFP contributed to the methodology, supervision of the clinical aspect of the study, data curation, acquisition, analysis, interpretation, supervision of the study, redaction, revision, and final approval of the manuscript. MD contributed to the conceptualization and design of the study, protocol development, methodology, data curation, acquisition, analysis, statistics, interpretation, supervision of the study, redaction, revision, and final approval of the manuscript.

Declarations

Competing interests

The authors declare no competing interests.

Additional information

Supplementary Information The online version contains supplementary material available at https://doi.org/10.1038/s41598-025-04271-2.

Correspondence and requests for materials should be addressed to R.A.C. or M.D.

Reprints and permissions information is available at www.nature.com/reprints.

Publisher's note Springer Nature remains neutral with regard to jurisdictional claims in published maps and institutional affiliations.